



# Synthesis, Characterization, Spectral Analysis and Molecular Simulation Studies of Compounds Formed by 2-mercaptopyridine and 1,4-dioxane Ligands with Some Metal (II) Chlorides

Zeki KARTAL<sup>1</sup> , Zarife Sibel SAHIN<sup>2,\*</sup> 

<sup>1</sup>Retired Professor of Atomic and Molecular Physics, TR-43020, Kütahya, Türkiye

<sup>2</sup>Sinop University, Faculty of Engineering and Architecture, Department of Energy Systems Engineering, TR-57000, Sinop, Türkiye

## Highlights

- $[\text{NiCl}_2(2\text{PS})_2]$  and  $[\text{CdCl}_2(\text{pD})_n]$  compounds were synthesized.
- These compounds have been experimentally characterized.
- The molecular modelling studies were carried out with DFT method.

## Article Info

Received: 13 Sep 2023

Accepted: 05 Apr 2024

## Keywords

2-mercaptopyridine  
2-pyridinethiolate  
1,4-dioxane  
molecular simulation  
SC-XRD analysis

## Abstract

In this investigation, two novel coordination compounds in crystalline form were synthesized utilizing chemical substances including 2-mercaptopyridine (2MP), 1,4-dioxane (pD), nickel(II) chloride ( $\text{NiCl}_2$ ), and cadmium(II) chloride ( $\text{CdCl}_2$ ), followed by an exploration of their structural properties through various experimental techniques. In addition, molecular modelling studies were carried out with B3LYP/LanL2DZ level using Gaussian 03 program. HOMO and LUMO orbitals, NBO studies were obtained by computation. The results from both experimental and optimized structural data were consistent. In particular, the vibration frequencies obtained experimentally of these compounds and the vibration frequencies theoretically calculated with B3LYP/LanL2DZ are substantially compatible with each other.

## 1. INTRODUCTION

Some of the coordination compounds (CCs) are formed by the continuous repetition of a certain structure in 1, 2 or 3 dimensions [1]. Such structures are called coordination polymers (CPs). The CPs, like some other compounds, has become the most interesting compounds of recent times due to of their gas storage, luminescence properties and magnetic properties [2,3]. It is thought that the CPs will be the most used structures in the coming years with their interesting and beneficial properties known so far, as well as new features that emerge day by day. Besides, various interactions are expected in the newly formed compound, depending on many factors such as the structural geometry of the newly formed compound, the presence of  $\pi$ - $\pi$  interactions in the ligands and co-ligands, and the presence or absence of the complementary atom in the pyridine ring of the ligands. The role of such interactions is very important in the crystal packing of the newly formed compound [1-3].

In this study, two different types of 2-mercaptopyridine (2MP) and 1,4-dioxane (pD) ligand molecules and  $\text{NiCl}_2$  and  $\text{CdCl}_2$  compounds were used to obtain new type of coordination polymers. 2MP; It is an organic sulfur compound with the closed formula  $\text{C}_5\text{H}_5\text{NS}$ , consisting of an SH group attached to a pyridine ring [4]. 2MP is a ligand molecule that can make between 1 and 3 bonds depending on the physical and chemical conditions of the environment. There are some scientific studies related to it by various researchers [5-13]. The pD is a heterocyclic organic compound classified as ether, with the closed formula  $\text{C}_4\text{H}_8\text{O}_2$ , normally

\*Corresponding author, e-mail: zarifesibel@sinop.edu.tr

in a colorless liquid state. The pD has a centrosymmetric structure and is generally found in the chair conformation in liquid form and its compounds. However, since it has a flexible structure, it can be found in the boat formation in its some compounds. Other isomers of pD (oD and mD) are rare and all are commonly used as solvents in organic chemistry. In addition to being used as solvents in organic chemistry, the pD, oD and mD compounds were used as ligands to obtain new compounds at the same time. There are many scientific studies on this subject, both by us and other researchers [14-27].

Nickel(II) chloride is a chemical compound consisting of a nickel and two chlorine atoms, represented by the formula  $\text{NiCl}_2$ . The color of nickel chloride changes depending on the number of water molecules in its structure. While the color of the anhydrous  $\text{NiCl}_2$  salt is yellow, the color of the most used and more known  $\text{NiCl}_2 \cdot 6\text{H}_2\text{O}$  compound is green. Various forms of Nickel(II) chloride are used as a source of nickel in the formation of chemical compounds. Various nickel salts increase the risk of developing cancer for living things that interact with them for a long time [28,29].

The ionic compound formed by the covalent bond of cadmium and chlorine atoms is called "Cadmium(II) chloride" and is represented by the formula  $\text{CdCl}_2$ . This compound is a crystalline chemical substance that is well soluble in water.  $\text{CdCl}_2$  is used in the synthesis of organocadmium compounds, ketones and many other chemical compounds in addition to its uses such as photocopying, painting and electroplating [30-34].

In this study, chemical synthesis of compounds with closed formulas as  $\text{NiCl}_2(2\text{MP})_2$  and  $\text{CdCl}_2(\text{pD})$  obtained in crystal form and their characterizations by various spectroscopic methods are given. The theoretical vibrations of the crystals obtained were calculated with the help of their .cif files at B3LYP/LanL2DZ level using the Gaussian 03 program [35]. The values of all calculated vibration frequencies are positive. These vibration frequencies were scaled with the appropriate coefficient and these values were found to be compatible with experimental values [36]. All kinds of visual pictures of the compounds were obtained with the help of GaussView 4.1 program [37].

## 2. MATERIAL METHOD

### 2.1. Materials

Some chemicals such as  $\text{NiCl}_2 \cdot 6\text{H}_2\text{O}$  (Alpha Aesar, 98%), 2-mercaptopyridine (2MP) ( $\text{C}_5\text{H}_5\text{NS}$ , Alpha Aesar, 98%),  $\text{CdCl}_2$  (Alpha Aesar, 99+%), 1,4-Dioxane (pD) ( $\text{C}_4\text{H}_8\text{O}_2$ , Sigma-Aldrich,  $\geq 99.0\%$ ), ethyl alcohol ( $\text{CH}_3\text{CH}_2\text{OH}$ , Alpha Aesar, Pure, 95.0%) and  $\text{NH}_4\text{OH}$  (Alpha Aesar, 25%  $\text{NH}_3$  in  $\text{H}_2\text{O}$ ) were used for synthesis. All chemicals required for the desired compounds were used without any additional treatment.

The infrared spectra of **1** and **2** were performed between  $3500 - 400 \text{ cm}^{-1}$  from KBr pellets on. Suitable crystals were selected for the structural characterization of **1** and **2** compounds. The data of the crystals were collected by using D8-QUEST diffractometer using  $\text{Mo-K}_\alpha$  radiation. The SHELXS-97 program [38] was used for the solutions of the structures. The SHELXL-97 program [38] within the WINGX [39] software was used in the refinement of the solved structures. The refinement was performed by using the least squares and the difference-Fourier methods. The C-H bond length is fixed at  $0.97 \text{ \AA}$  by using the riding model in the refinement of the hydrogen atoms. The molecular diagrams of the structures were drawn by the MERCURY program [40]. Table 1 provides the specifics regarding data collection and refinement.

### 2.2. Syntheses of the $\text{NiCl}_2(2\text{MP})_2$ and $\text{CdCl}_2(\text{pD})$ Compounds

To obtain the compound  $\text{NiCl}_2(2\text{MP})_2$ ; 1 mmol of  $\text{NiCl}_2 \cdot 6\text{H}_2\text{O}$  (237.69 g) was dissolved in 10 mL of hot distilled water. Then, 2 mmol of 2MP, (222.32 g) dissolved in 5 mL of hot ethyl alcohol was added dropwise into this solution. The mixture was stirred for 3 hours at  $65 \text{ }^\circ\text{C}$  and a stirring speed of 750 rpm. It was observed that the light green colored  $\text{NiCl}_2(2\text{MP})_2$  compound was formed as a suspension in a mixture of ethyl alcohol and water. Later, aqueous  $\text{NH}_3$  solution was slowly added to the reaction. This mixture was then filtered. After about six weeks, colorless, transparent crystals thought to have the chemical formula  $\text{NiCl}_2(\text{C}_5\text{H}_5\text{NS})_2$  (compound **1**) were obtained.

To obtain the compound CdCl<sub>2</sub>(pD); 1 mmol of CdCl<sub>2</sub> anhydrous (0.183 g) was dissolved in 10 mL of hot distilled water. Then, 1 mmol of pD, (0.089 g) dissolved in 5 mL of hot ethyl alcohol was added dropwise into this solution. Later, the method applied for mixture 1 was repeated for mixture 2 and [CdCl<sub>2</sub>(C<sub>4</sub>H<sub>8</sub>O<sub>2</sub>)<sub>n</sub>] (compound **2**) were obtained.

**Table 1.** Experimental parameters for compounds **1** and **2**

	<b>1</b>	<b>2</b>
Empirical formula	C <sub>10</sub> H <sub>8</sub> Cl <sub>2</sub> N <sub>2</sub> NiS <sub>2</sub>	C <sub>4</sub> H <sub>8</sub> Cl <sub>2</sub> CdO <sub>2</sub>
Formula weight	349.91	271.40
Crystal system	Orthorhombic	Monoclinic
Space group	<i>Fdd2</i>	<i>C2/m</i>
<i>a</i> (Å)	12.8473 (10)	7.615 (2)
<i>b</i> (Å)	27.557 (3)	11.967 (3)
<i>c</i> (Å)	8.1463 (6)	3.8612 (9)
$\beta$ (°)	90.00	93.224 (9)
<i>V</i> (Å <sup>3</sup> )	2884.0 (4)	351.31 (16)
<i>Z</i>	8	2
<i>D<sub>c</sub></i> (g cm <sup>-3</sup> )	1.612	2.566
$\theta$ range (°)	4.3-30.5	3.2-28.3
Measured refls.	10341	7092
Independent refls.	1786	458
<i>R</i> <sub>int</sub>	0.048	0.032
<i>S</i>	1.10	1.20
<i>R</i> <sub>1</sub> / <i>wR</i> <sub>2</sub>	0.070/0.211	0.012/0.028
$\Delta\rho_{\max}/\Delta\rho_{\min}$ (eÅ <sup>-3</sup> )	2.05/-0.96	0.42/-0.43
CCDC	2069757	2060795

The amounts of nickel and cadmium metals were analyzed by Perkin-Elmer optima 4300 DV ICP-OES, and the C, N, S and H amounts were analyzed by CHNS-932 (LECO). Experimental results obtained from these measurements and theoretically calculated results for compounds **1** and **2** are given below, respectively.

For compound **1**:

Experimentally found (%): C, 34.23; H, 2.36; Ni, 16.85; N, 8.13; S, 18.19.

Theoretically calculated (%): [C<sub>10</sub>H<sub>10</sub>Cl<sub>2</sub>N<sub>2</sub>NiS<sub>2</sub>, (M<sub>r</sub> = 351.93 g / mol)]: C, 34.13; H, 2.86; Ni, 16.68; N, 7.96; S, 18.22.

For compound **2**:

Experimentally found (%): C, 17.91; H, 2.71; Cd, 42.12.

Theoretically calculated (%): [C<sub>4</sub>H<sub>8</sub>CdCl<sub>2</sub>O<sub>2</sub>, (M<sub>r</sub> = 271.89 g / mol)]: C, 17.70; H, 2.97; Cd, 41.62.

It is seen that there are some discrepancies between the theoretical and experimental results of compound **1**, especially in hydrogen percentages. This situation can be evaluated as a normal result that occurs between the current information and two different methods.

However, when examining the crystal data regarding the structure of compound **1**, it is seen that the 2MP molecule has lost hydrogen in compound **1**. This new situation for the 2MP molecule is a new structure

called "2-Pyridinethiolate" (2PS). According to the results of this new situation, the discrepancy between the theoretical and experimental analyzes of compound **1** disappears. In this case, the closed formula of compound **1** must be in the form of  $\text{NiCl}_2(2\text{PS})_2$ . Necessary information on this subject will be given in the spectral examination of compound **1** section.

The theoretical analysis values of compound **1** in this case are as follows.

Theoretically calculated for compound **1** (%):  $[\text{C}_{10}\text{H}_8\text{Cl}_2\text{N}_2\text{NiS}_2, (\text{M}_r = 349.91 \text{ g/mol})]$ : C, 34.33; H, 2.30; Ni, 16.77; N, 8.01; S, 18.33.

It is seen that the newly obtained theoretical values for compound **1** are quite compatible with the experimental values.

### 3. THE RESEARCH FINDINGS AND DISCUSSION

#### 3.1. Crystallographic Studies of Compounds **1** and **2**

##### Compound **1**

The molecular diagram of compound **1** obtained from XRD results is given in Figure 1. The compound **1** contains one coordinated chlorine atom, one Ni(II) ion and one 2PS ligand in the asymmetric unit. The Ni(II) ion is attached to two S atoms  $[\text{Ni1-S1} = 2.517(4) \text{ \AA}]$  from 2PS ligands and two Cl atoms  $[\text{Ni1-Cl1} = 2.473(4) \text{ \AA}]$ , therefore displaying a distorted tetrahedral geometry. Ni-Cl and Ni-S bond lengths were presented as 2.3866(4), 2.4208(8) and 2.172(8)  $\text{\AA}$  in similar studies [41, 42, 43].

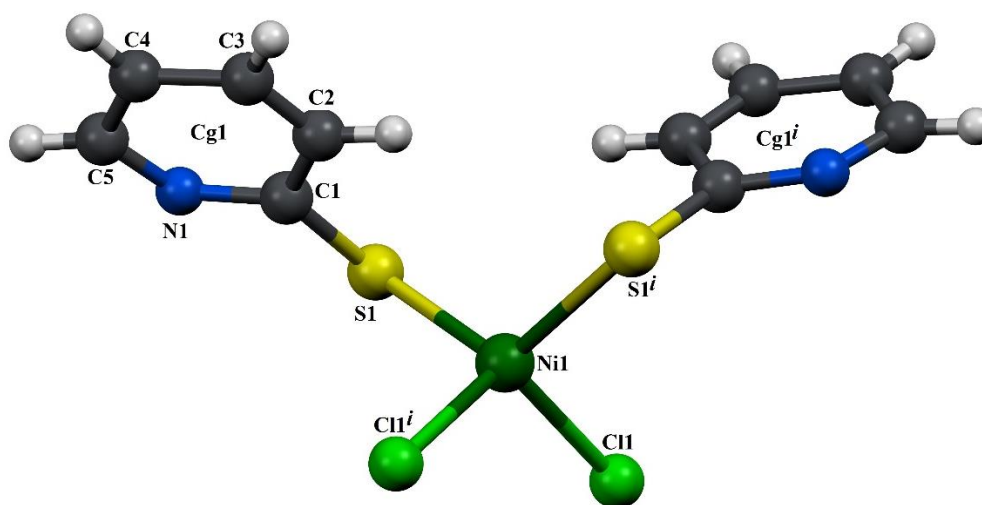


**Figure 1.** Compound **1**'s molecular configuration

The 2PS molecules in the structure of compound **1** are linked together by  $\pi \cdots \pi$  interactions (Figure 2). A  $\pi \cdots \pi$  interactions occur between the two pyridine rings (Cg1) associated with the symmetries of neighboring 2PS ions. These interactions hold all compounds **1** molecule together. The Cg1-Cg1<sup>i</sup> perpendicular distance is 3.4720  $\text{\AA}$   $[(i) 1/4+x, 3/4-y, -1/4+z]$ . The distance between the centers of pyridine rings interacting with each other is 3.8389  $\text{\AA}$ .

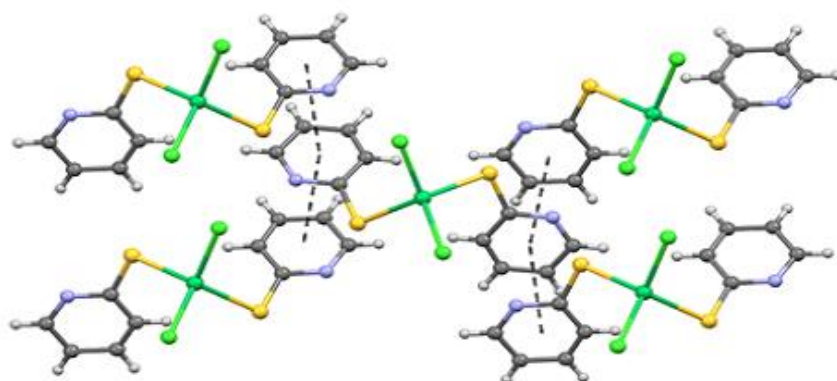


**Figure 2.** Crystal packing of compound **1**, showing the chain formation resulting from the  $\pi\cdots\pi$  interactions of pyridine rings

### Compound 2

Looking at the structure of compound **2**, it is seen that it forms a 2D coordination polymer (Figure 4). The compound **2** contains one coordinated chlorine atom, one Cd(II) ion, and a half pD ligand in the asymmetric unit (Figure 3). The Cd(II) ion is attached to two O atoms [Cd1-O1 = 2.4235(16) Å] from pD ligands, and four Cl atoms [Cd1-Cl1 = 2.6010(6) Å], therefore displaying a distorted octahedral geometry. Cd-Cl and Cd-O bond lengths were presented as 2.582 and 2.372(7) Å, respectively in similar studies [44, 45]. The pD ligands and the Cd(II) ions form a 1D coordination polymer running parallel to the [100] direction. Adjacent these polymers are joined by chlorine atoms, with grid dimensions are  $3.861 \times 7.615$  Å (Figure 4) (defined by Cd···Cd distances). The unit cells of compounds **1** (a) and **2** (b) are shown in Figure 5, respectively. Table 2 shows some selected bond lengths and angles for both molecules.

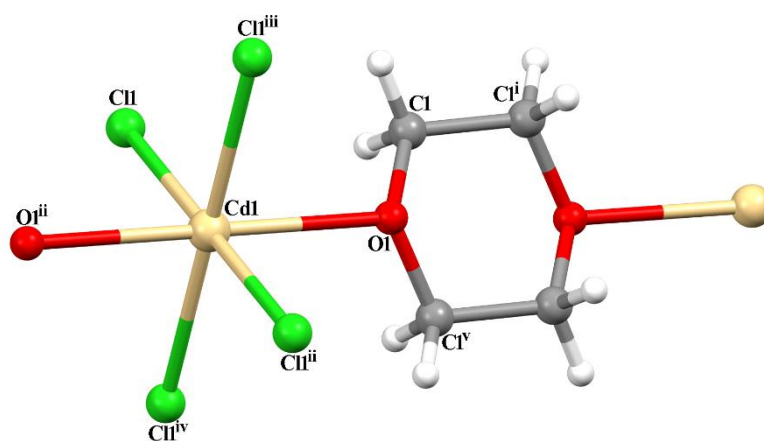


**Figure 3.** Compound **2**'s molecular configuration

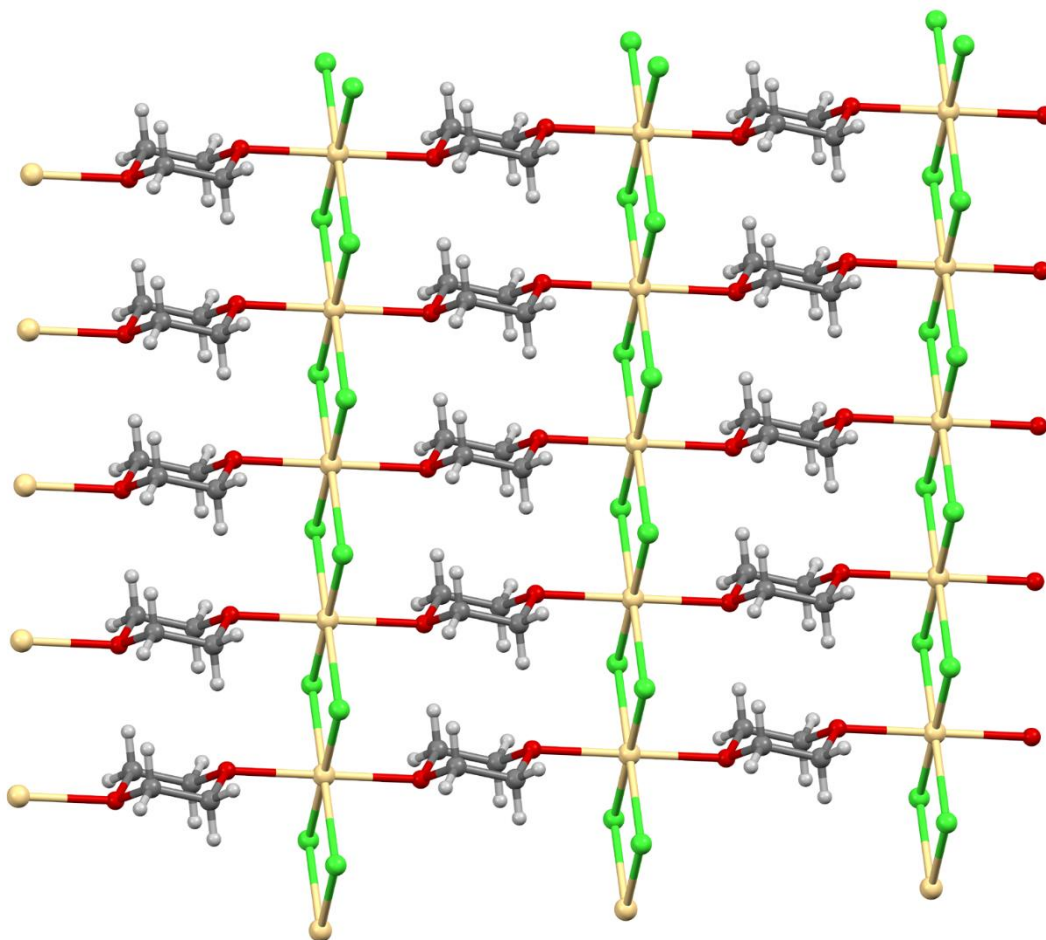


Figure 4. An infinite 2D layer in compound 2

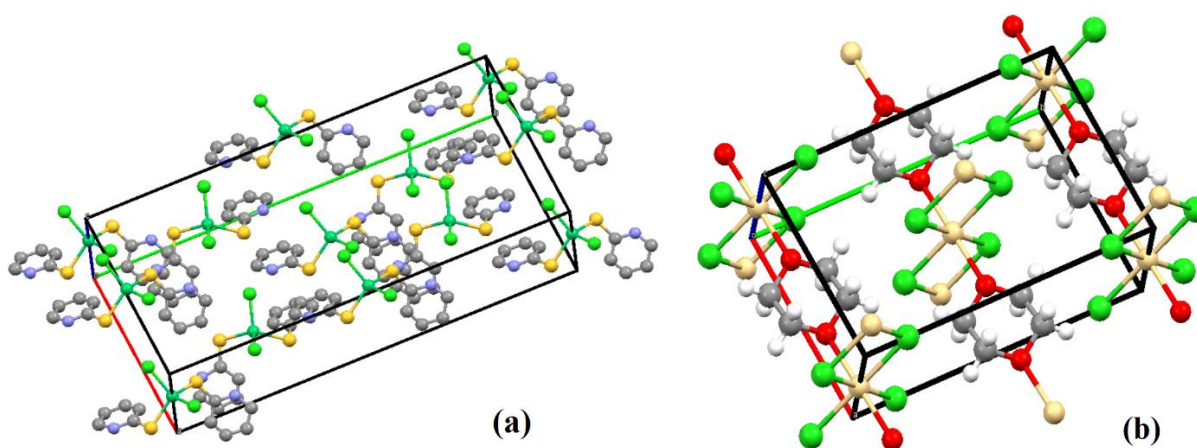


Figure 5. The unit cells of compounds 1 (a) and 2 (b)

Table 2. Comparison of some selected geometric parameters of compounds 1 and 2 ( $\text{\AA}$ ,  $^\circ$ )

Compound 1			Compound 2		
	XRD	LanL2DZ		XRD	LanL2DZ
Ni1-Cl1	2.473 (4)	1.191	Cd1-O1	2.4235(16)	2.278
Cl1-Ni1-Cl1 <sup>i</sup>	115.2(2)	157.452	Cd1-Cl1	2.6010(6)	2.417
Cl1-Ni1-S1	100.86(12)	93.494	O1-Cd1-Cl1 <sup>ii</sup>	87.55(3)	100.818

Ni1-S1	2.517 (4)	2.257	C11-Cd1-C11 <sup>iii</sup>	84.15(3)	-
C11-Ni1-S1 <sup>i</sup>	109.76(13)	101.607	O1-Cd1-C11	92.45(3)	100.818
S1-Ni1-S1 <sup>i</sup>	121.1(2)	95.810	C11-Cd1-C11 <sup>iv</sup>	95.85(3)	-

Symmetry codes: (i)  $-x+1, -y+1, z$  for **1**; (ii)  $-x+1, -y+1, -z+1$ ; (iii)  $-x+1, -y+1, -z$ ; (iv)  $x, y, z+1$  for **2**

### 3.2. Computational Studies

Apart from the geometric and spectroscopic properties of the two synthesized molecules, some physicochemical properties, atomic charges, natural bond orbital analyses, HOMO-LUMO energies, some chemical parameters and thermodynamic properties were also investigated theoretically. The molecular geometries of the compounds were taken from their X-ray diffraction results for theoretical calculations. DFT/B3LYP method was chosen as the computational method and Gaussian 03 program was used. LanL2DZ was chosen as the basis set because it gives meaningful energy values and suitable geometry [35]. The molecular diagrams of the optimized structures for molecules **1** and **2** are given in Figure 6 (a) and (b). Compound **1** and compound **2**'s geometric parameters were computed using the DFT method at the B3LYP/ LanL2DZ level and documented in Table 2, alongside their experimental counterparts. Notably, the optimized bond lengths generally deviate slightly from the experimental data due to differences in molecular states between experimental and theoretical contexts. Experimental measurements typically involve molecules within condensed phases, while theoretical calculations often focus on isolated molecules in the gas phase.

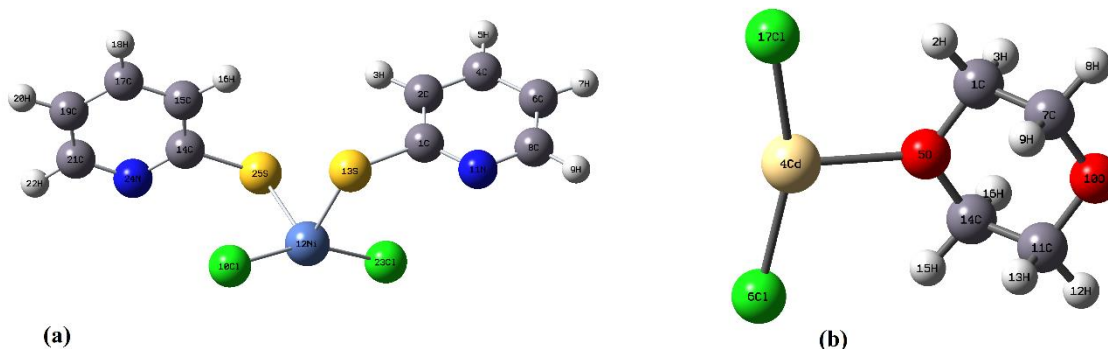


**Figure 6.** Optimized geometry of molecules **1**(a) and **2**(b) calculated by DFT/B3LYP method

#### Mulliken atomic charges:

The electrical charges on each atom of a chemical compound that has reached a stable structure are also called "Mulliken charges". The Mulliken charges are widely used because they provide a rough general idea about the molecule's polarity, its electronic structure, atom charge distribution as well as donor and acceptor pairs within the molecules. Figure 7 illustrates the Mulliken atomic charges for molecules **1** and **2**, calculated using B3LYP/ LanL2DZ. As depicted in Figure 7, the charges of all hydrogen atoms in both compounds are of a positive value. All carbon atoms in compound **2** have negative charge values. While all chlorine and oxygen atoms in compound **2** have negative charge values, cadmium atom has positive charge value. While 13 S atom in compound **1** and 17 Cd atom in compound **2** have the largest positive charge values, the smallest negative charge values are 23 Cl atom in compound **1** and 14 O atom in compound **2**.

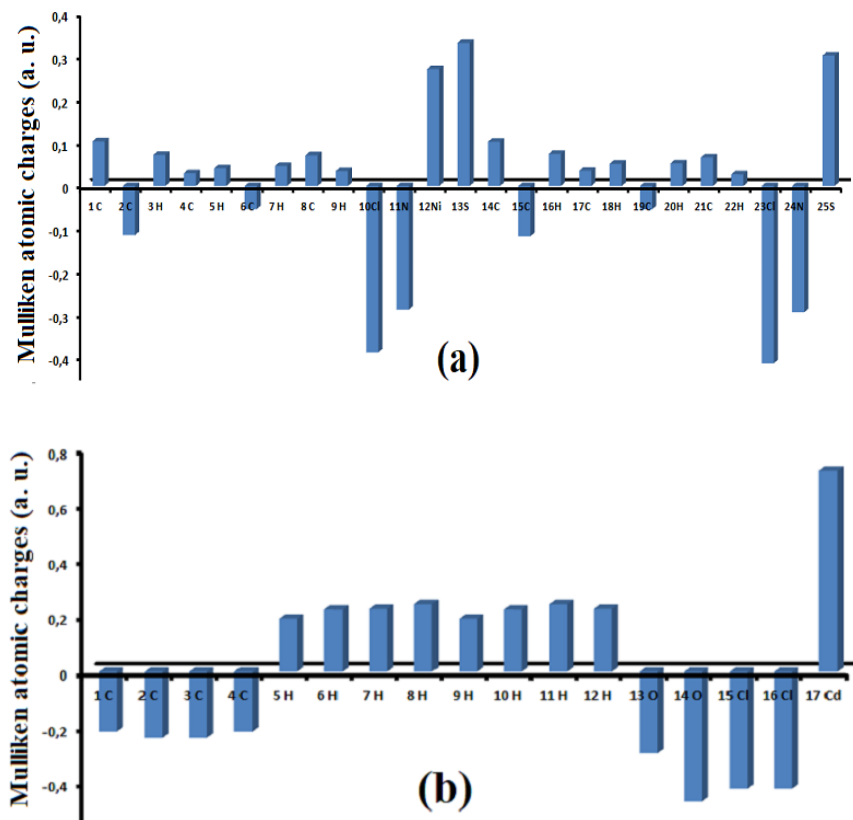
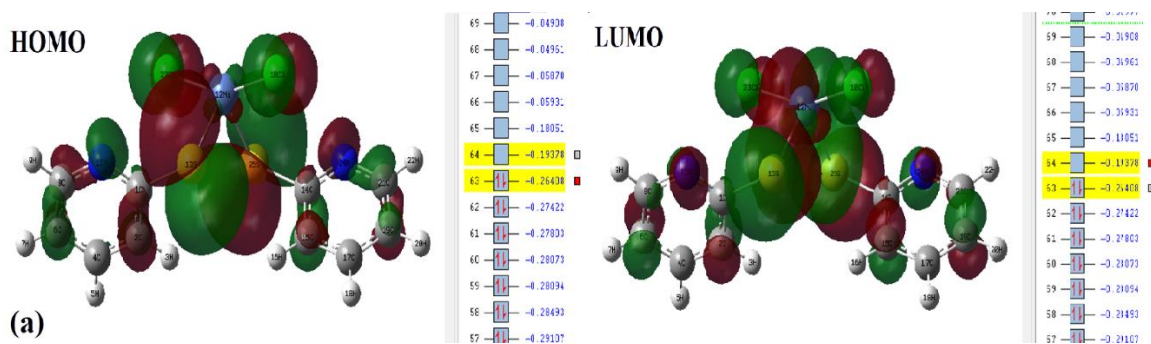


Figure 7. The Mulliken charge distribution in compounds 1 (a) and 2 (b)

### Frontier Molecular Orbitals:

The HOMO-LUMO molecular orbitals are of great importance in understanding the optical and electronic properties of molecules. HOMO and LUMO orbitals are considered boundary molecular orbitals where a molecule interacts with other molecules. HOMO energy refers to the potential to donate electrons, LUMO energy refers to the potential to gain electrons, and the energy gap between the two refers to the chemical stability of the molecule. The frontier molecular orbitals for compounds 1 and 2 have been calculated by the DFT/B3LYP method and the LanL2DZ basis set and Figure 8 shows energy levels of frontier molecular orbitals.





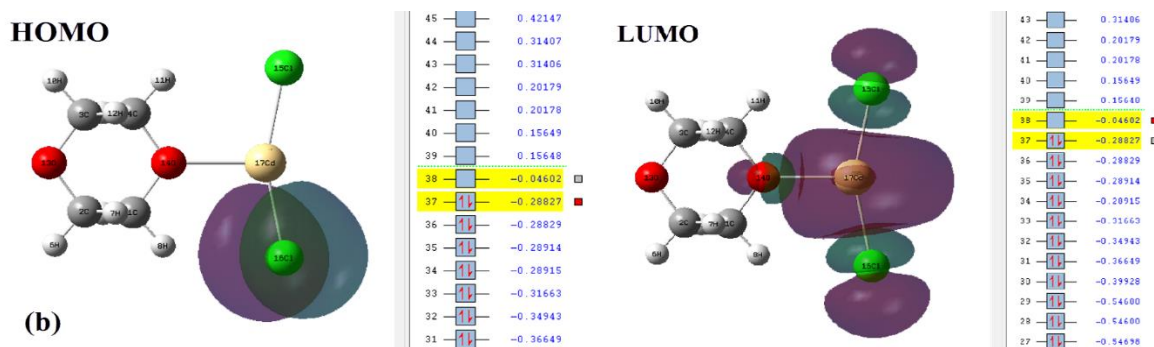


**Figure 8.** The frontier molecular orbitals of compounds **1** (a) and **2** (b)

The energy gap between the HOMO and LUMO orbitals not only characterizes the chemical stability of the molecule but also signifies the extent of charge transfer occurring within it. The energy gap determines the energy required within the molecule to move from the ground state to an excited state. As seen in Figure 8, the HOMO and LUMO energy values for **1** were  $-0.26194$  a.u. ( $-7.128$  eV) and  $-0.22316$  a.u. ( $-6.072$  eV), respectively. Similarly, while the HOMO energy value of compound **2** is  $-0.28827$  a.u. ( $-7.844$  eV), LUMO energy value is  $-0.04602$  a.u. ( $-1.252$  eV). As the HOMO–LUMO energy gap ( $\Delta E$ ) increases in a molecule, the molecule becomes more stable and less reactive; conversely, reducing this energy gap makes the molecule more susceptible to chemical reactions, destabilizing it and lowering the threshold energy for reactions. The energy differences between the HOMO and LUMO for molecules **1** and **2** are  $1.056$  eV and  $6.592$  eV, respectively. Therefore, we can say that molecule **2**, which has a larger energy gap, will be more stable and non-reactive than molecule **1**.

Using HOMO-LUMO energies, some physicochemical parameters such as chemical softness ( $S$ ), electrophilicity index ( $\omega$ ), chemical potential ( $\mu$ ), electronegativity ( $\chi$ ), and chemical hardness ( $\eta$ ) indicating the chemical activities of the molecules were also calculated. These values for molecules **1** and **2** are given in Table 3. When we examine Table 3, we can say that molecule **2** will be more stable than molecule **1**. At the same time, the higher chemical potential and lower chemical hardness value of molecule **1** indicate that it will exhibit a better electrophilic character than compound **2**. The same situations have been reported in similar studies [46, 47].

**Table 3.** The HOMO and LUMO energies and chemical parameters of compounds **1** and **2**

	HOMO (eV)	LUMO (eV)	$\Delta E$ (eV)	$\chi$ (eV)	$\mu$ (eV)	$\eta$ (eV)	$S$ (eV) <sup>-1</sup>	$\omega$ (eV) <sup>-1</sup>
Compound <b>1</b>	-7.128	-6.072	1.056	6.600	-6.600	0.528	0.94697	41.250
Compound <b>2</b>	-7.844	-1.252	6.592	4.548	-4.548	3.296	0.15170	3.138

### Thermodynamic parameters:

Heat production, which is a thermochemical property for any compound, is one of the most important thermochemical parameters of that compound. For most organic compounds their heat generation values are unknown. The fact that it is very difficult to experimentally examine the heat effects of compounds increases the importance of quantum chemical calculations in this regard. Thermodynamically, it can be decided whether a chemical reaction will take place by examining the effect of heat. The thermochemical properties calculated for both compound **1** and compound **2** are given in Table 4.

As a result, it is observed that the compound **1**'s all thermal chemical values are greater than the thermal chemical values of compound **2**. This result reveals the fact that compound **1** has better heat storage property and better heat dissipation property than compound **2**.

**Table 4.** Thermochemical data of compounds **1** and **2**

	Compound 1	Compound 2
<b>E<sub>Total</sub> (kcal/mol)</b>	<b>113.98</b>	<b>86.08</b>
Electronic	0.000	0.000
Translational	0.889	0.889
Rotational	0.889	0.889
Vibrational	112.205	84.304
<b>C<sub>v</sub> Heat Capacity at constant volume (cal/mol.K)</b>	<b>61.84</b>	<b>36.97</b>
Electronic	0.000	0.000
Translational	2.981	2.981
Rotational	2.981	2.981
Vibrational	55.883	31.010
<b>S Total entropy (cal/mol.K)</b>	<b>148.24</b>	<b>112.55</b>
Electronic	0.000	0.000
Translational	43.434	42.700
Rotational	34.391	31.857
Vibrational	70.415	37.991
<b>E<sub>v0</sub> Zero point Vibration Energy (kcal/mol)</b>	<b>102.60</b>	<b>78.94</b>
<b>Rotational constants (GHz)</b>		
A	0.52157	0.97393
B	0.17209	0.52209
C	0.15664	0.35398

**Natural bond orbital analysis:**

To better understand the intramolecular-intermolecular interactions and the interactions between the bonds, NBO analysis was performed on optimized structures. In molecules with a higher  $E^{(2)}$  value, interactions among electron-donating and -accepting sites are more dominant. In this case, the structure is more stable. Table 5 gives the types of donor-acceptor interactions, and their perturbation energy values for compounds **1** and **2**.

As a result, it can be said that compound **1** exhibits higher energy values for charge transitions compared to compound **2**, both in terms of the number of transitions and their respective values. This result is evidence that compound **1** is more active than compound **2** in terms of its thermochemical properties.

**Table 5.** Second order perturbation theory analysis of Fock matrix on NBO of compounds **1** and **2**

Donor NBO (i)	Acceptor NBO (j)	$E^{(2)a}$ (kcal/mol)	$E(j)-E(i)^b$ (a.u.)	$F(i,j)^c$ (a.u.)
<b>Compound 1</b>				
LP (4) Ni 12	LP* (3) S 13	121.02	0.03	0.069
$\pi^*$ (C 1-N 11)	$\pi^*$ (C 6-C 8)	86.00	0.03	0.080
$\pi^*$ (C 14-N 24)	$\pi^*$ (C 19-C 21)	86.00	0.03	0.080
LP (4) Cl 10	LP* (5) Ni 12	85.61	0.42	0.172
LP (4) Cl 23	LP* (5) Ni 12	85.43	0.42	0.172
$\pi^*$ (C 14-N 24)	$\pi^*$ (C 15-C 17)	83.78	0.04	0.085
$\pi^*$ (C 1-N 11)	$\pi^*$ (C 2-C 4)	83.78	0.04	0.085
$\sigma^*$ (Ni 12-S 25)	LP* (5) Ni 12	72.40	0.29	0.175
LP* (3) S 13	LP* (5) Ni 12	36.74	0.38	0.118
$\sigma$ (Ni 12-S 25)	LP* (3) S 13	36.54	0.08	0.064
LP* (5) Ni 12	RY* (8) Ni 12	30.03	1.68	0.406
$\pi$ (C 1-N 11)	LP* (3) S 13	28.88	0.05	0.045
$\pi$ (C 15-C 17)	$\pi^*$ (C 14-N 24)	28.83	0.24	0.076
$\pi$ (C 2-C 4)	$\pi^*$ (C 1-N 11)	28.83	0.24	0.076
$\pi$ (C 1-N 11)	$\pi^*$ (C 6-C 8)	22.28	0.33	0.076
$\pi$ (C 14-N 24)	$\pi^*$ (C 19-C 21)	22.28	0.33	0.076
$\pi$ (C 19-C 21)	$\pi^*$ (C 14-N 24)	21.45	0.24	0.065
$\pi$ (C 6-C 8)	$\pi^*$ (C 1-N 11)	21.45	0.24	0.065
$\pi$ (C 6-C 8)	$\pi^*$ (C 2-C 4)	20.60	0.28	0.070
$\pi$ (C 19-C 21)	$\pi^*$ (C 15-C 17)	20.60	0.28	0.070
$\pi$ (C 15-C 17)	$\pi^*$ (C 19-C 21)	19.84	0.28	0.068

$\pi$ (C 2-C 4)	$\pi^*$ (C 6-C 8)	19.84	0.28	0.068
LP (2) Cl 23	LP* (5) Ni 12	16.01	0.50	0.091
LP (2) Cl 10	LP* (5) Ni 12	15.99	0.50	0.091
LP* (5) Ni 12	RY* (6) Ni 12	14.94	0.87	0.206
$\pi$ (C 14-N 24)	$\pi^*$ (C 15-C 17)	14.87	0.33	0.063
$\pi$ (C 1-N 11)	$\pi^*$ (C 2-C 4)	14.87	0.33	0.063
$\sigma$ (Ni 12-S 25)	LP (4) Ni 12	14.22	0.05	0.037
LP* (3) S 13	$\pi^*$ (C 1-N 11)	13.68	0.24	0.058
LP (1) N 11	$\sigma^*$ (C 1-C 2)	11.81	0.83	0.090
LP (1) N 24	$\sigma^*$ (C 14-C 15)	11.81	0.83	0.090
LP (2) S 13	$\sigma^*$ (Ni 12-S 25)	11.75	0.09	0.032
LP (3) Cl 10	LP* (3) S 13	11.33	0.02	0.017
LP (1) N 24	$\sigma^*$ (C 19-C 21)	10.37	0.84	0.085
LP (1) N 11	$\sigma^*$ (C 6-C 8)	10.37	0.84	0.085
<b>Compound 2</b>				
LP (4) Cl 15	$\sigma^*$ (Cl 16-Cd 17)	48.24	0.30	0.108
LP (2) O 14	$\sigma^*$ (Cl 16-Cd 17)	10.21	0.62	0.074
LP (4) Cl 15	RY* (2) Cd 17	6.69	0.72	0.065
LP (2) O 13	$\sigma^*$ (C 1-C 2)	5.30	0.63	0.052
LP (2) O 13	$\sigma^*$ (C 3-C 4)	5.30	0.63	0.052
$\sigma$ (C 3-H 10)	$\sigma^*$ (C 4-O 14)	5.13	0.70	0.054
$\sigma$ (C 2-H 6)	$\sigma^*$ (C 1-O 14)	5.13	0.70	0.054
LP (2) O 13	$\sigma^*$ (C 3-H 9)	4.94	0.74	0.054
LP (2) O 13	$\sigma^*$ (C 2-H 5)	4.94	0.74	0.054
LP (1) Cl 15	$\sigma^*$ (Cl 16-Cd 17)	4.56	0.64	0.051
$\sigma$ (C 4-H 11)	$\sigma^*$ (C 3-O 13)	4.31	0.76	0.051
$\sigma$ (C 1-H 8)	$\sigma^*$ (C 2-O 13)	4.31	0.76	0.051
$\sigma^*$ (Cl 16-Cd 17)	RY* (12) Cd 17	4.08	2.58	0.269
$\sigma$ (C 3-H 10)	$\sigma^*$ (C 2-O 13)	4.07	0.75	0.049
$\sigma$ (C 2-H 6)	$\sigma^*$ (C 3-O 13)	4.07	0.75	0.049
LP (1) O 14	$\sigma^*$ (C 4-H 12)	4.03	0.80	0.051
LP (1) O 14	$\sigma^*$ (C 1-H 7)	4.03	0.80	0.051
$\sigma$ (C 4-H 11)	$\sigma^*$ (C 1-O 14)	3.86	0.71	0.047
$\sigma$ (C 1-H 8)	$\sigma^*$ (C 4-O 14)	3.86	0.71	0.047
$\sigma^*$ (Cl 16-Cd 17)	RY* (10) Cd 17	3.78	1.56	0.201
LP (4) Cl 15	RY* (12) Cd 17	3.68	2.89	0.098
LP (1) O 14	$\sigma^*$ (C 3-C 4)	3.34	0.68	0.043
LP (1) O 14	$\sigma^*$ (C 1-C 2)	3.34	0.68	0.043
LP (4) Cl 15	RY* (10) Cd 17	3.18	1.87	0.073
$\sigma$ (C 3-H 9)	$\sigma^*$ (C 4-H 12)	3.06	0.98	0.049
$\sigma$ (C 2-H 5)	$\sigma^*$ (C 1-H 7)	3.06	0.98	0.049

<sup>a</sup>  $E^{(2)}$  means energy of hyperconjugative interaction (stabilization energy),

<sup>b</sup> Energy difference between donor and acceptor i and j NBO orbitals,

<sup>c</sup>  $F(i, j)$  is the Fock matrix element between i and j NBO orbital,

<sup>d</sup> Stared label (\*) indicates anti-bonding, LP (A) is a valence lone pair orbital on atom A and RY\* for 1-center Rydberg.

### 3.3. Spectral Analysis

To compare with the experimental vibration data of both compound **1** and compound **2**, their vibration modes were calculated with Gaussian 03 program DFT/B3LYP method, LanL2DZ basis set [35]. Before comparing with experimental values, the theoretical values were multiplied by 0.958 coefficients for wavenumbers larger than  $1700\text{ cm}^{-1}$  and by 0.988 coefficients for wavenumbers smaller than  $1700\text{ cm}^{-1}$ , respectively [36]. The fit equations between the experimental and scaled theoretical vibration values of compounds **1** and **2** were obtained as  $y_1 = 1.0543x_1 - 49.709$  ( $R^2 = 0.999$ ) and  $y_2 = 1.0602x_2 - 48.823$  ( $R^2 = 0.999$ ), respectively (Figure S1).

The vibration spectra of 2MP ligand and of the compound **1** are given in Figure S2. Similarly, experimental FT-IR spectra and theoretical vibration spectra of the liquid pD ligand and compound **2** are given in Figure S3. FT-IR spectral data obtained for compounds **1** and **2** were interpreted by considering the changes in the

vibrations of 2MP and pD ligand molecules and NiCl<sub>2</sub> and CdCl<sub>2</sub> units, one by one, resulting from compound formation.

When the spectra of compounds **1** and **2** are examined carefully, it is seen that the FT-IR spectra of each compound are different from each other. Because the ligand molecules that make up both compounds are different from each other. Therefore, both compounds are expected to crystallize in different structures. The accuracy of this situation can be clearly seen from Table 1 and Figures 1-4.

The compounds **1** and **2** will be discussed separately for their spectroscopic properties, respectively.

### **Compound 1**

The 2MP molecule involved in the formation of compound **1** is an organic sulfur compound in the C1 conformation and space group P21/c which the pyridine ring and thiol (-SH) group are in the same plane. Since the 2MP molecule has 12 atoms, it has 30 vibration modes, all of which are both IR and Raman active.

The 2MP molecule that contributes to the formation of compound **1** can make three different bonds to metal atoms or other molecules due to its three different electron donor regions. The three different electron donating regions of 2MP are the S atom in the SH group, the N atom in the pyridine ring and the  $\pi$  electrons located in the pyridine ring, respectively.

Depending on the activity values of these electron donating regions, the 2MP molecule can make at least one bond and at most three bonds to metal atoms or other molecules around it [43]. Spectral data of the 2MP molecule and compound **1** are listed in Table S1.

From the review of Figure 1 and Table S1, it is understood that some significant changes occurred in the 2MP molecule during the formation of compound **1**. One of these changes is the disappearance of the SH stretching peak observed at 2507 cm<sup>-1</sup> wavenumber in the FT-IR spectrum of the solid state 2MP molecule. This situation was observed in aliphatic and aromatic sulfur compounds that we have previously examined and in similar studies of other researchers [44-48].

In the solid state, a pair of 2MP molecules usually exist in the form of dimer, linked together from hydrogen and sulfur atoms. This dimeric structure is called the "thion form" for thiols [5, 9, 10]. However, if the 2MP molecule is attached to a metal atom from the sulfur atom, the dimeric structure is broken. In this case, each 2MP molecule loses one hydrogen atom and takes the form of 2-pyrinethiolate [6, 49, 50]. The thiolate form of the 2MP molecule is structurally an anion, and it is denoted by the abbreviation 2PS. The 2-pyrinethiolate (2PS) structures can generally bond with other atoms in the compound in which they are located, either only from sulfur atoms or only from nitrogen atoms or from both sulfur and nitrogen atoms. Even, these thiolate structures interact with each other because of the  $\pi$  electrons in pyridine rings [9, 51, 52].

The experimental vibration spectrum of in solid state 2MP molecule and the theoretical and experimental vibration spectra of compound **1** should be examined together. The indicated examination for the 2MP molecule and compound **1** was made and the results are given in Table S1.

If there are symmetric structures or symmetric groups in a molecule or a compound, fewer vibration peaks appear in their experimental spectra than theoretical values. Because only one vibration peak is observed for each identical symmetric structures or symmetric groups in the molecule or compound studied theoretically.

As can be seen from Figure 6 (a), there are 25 atoms in compound **1**. According to theoretical calculation, it should have 69 vibration modes. However, 33 vibration modes have emerged in their experimental spectrum. The reason for this is that there are symmetrical and identical groups in its structure or the intensities of some vibration modes are quite small.

To support the experimental spectral data of compound **1** in Table S1, theoretical vibration calculations were made at the B3LYP/LanL2DZ level and the assignments of the vibration peaks were made with the VEDA 04 program [53].

It can be seen from the examination of Table S1 that some spectroscopic results for the formation of compound **1** have been obtained. These spectroscopic results can be listed as the changes in the vibration modes of 2MP due to its compound formation and the formation of new some vibration modes resulting from the bonding of 2MP with NiCl<sub>2</sub>. Some of these spectroscopic results are marked in bold and italic bold in Table S1 for easier viewing, respectively.

Looking at Table S1, the CH stretching vibrations in the solid state 2MP molecule shifted to the high frequency region by about 13-29 cm<sup>-1</sup> wavenumber in the 2PS thiolate form due to the formation of compound **1**. Because no hydrogen bond contributes to the formation of compound **1**, these shifts are only due to the change in the environmental conditions of 2PS. The reality of this situation is evident from Figure 1, Figure 2 and Figure 5 (a).

It is also seen that the in-plane and out-of-plane bending vibrations of the C-SH part of the 2MP molecule at the 911 and 212 cm<sup>-1</sup> wavenumbers disappear because of the transformation into the 2PS thiolate form.

Experimental studies about the vibration modes of NiCl<sub>2</sub> and NiCl<sub>2</sub>·6H<sub>2</sub>O compounds are given in references 28 and 29. In addition, the theoretical calculation of vibration modes was made with Gaussian 03 program for the case where Cl-Ni-Cl angle for NiCl<sub>2</sub> is 120°. According to this theoretical study, the asymmetric Ni-Cl stretching [*v*<sub>as</sub>(Ni-Cl)], symmetrical Ni-Cl stretching [*v*<sub>s</sub>(Ni-Cl)] and in-plane bending [*β*(Cl-Ni-Cl) ip] vibration modes calculated for free NiCl<sub>2</sub> were obtained at wavenumbers of 475, 388 and 80 cm<sup>-1</sup>, respectively. It has been seen that these values are compatible with the experimental values [28,29].

In the theoretical calculation for compound **1**, these vibration modes of NiCl<sub>2</sub> bonded to the structure were obtained as unscaled at 442, 304 and 82 cm<sup>-1</sup> wavenumbers, respectively.

### **Compound 2**

The pD molecule is a centrosymmetric molecule with a total of 14 atoms, a chair conformation and theoretically 36 vibration modes of which 14 are IR active, 15 are Raman active and 7 are both IR and Raman active. It has a structurally flexible structure and can easily pass into the boat conformation to form a chelate structure with metal atoms when necessary [54]. However, it is clear from Figures 3, 4 and 5 (b) that the pD molecule preserves the chair conformation in the structure of compound **2**.

Vibration bands of the pD molecule in liquid form and in the structure of compound **2** are given in Table S2. Compared to the liquid phase, these vibrations of pD show large variations for the resulting compound **2**. This result is naturally due to the compounding of pD with CdCl<sub>2</sub>. These results indicate that the interaction of pD with CdCl<sub>2</sub> is strong in compound **2**.

It can be seen from the examination of Table S2 that some spectroscopic results for the formation of compound **2** have been obtained. These spectroscopic results can be listed as the changes in the vibration modes of pD due to its compound formation and the formation of new some vibration modes resulting from the bonding of pD with CdCl<sub>2</sub>. Some of these spectroscopic results are marked in bold and italic bold in Table S2 for easier viewing, respectively.

Experimental studies of the vibration modes of CdCl<sub>2</sub> are given in references [55] and [56]. In addition, for the case where Cl-Cd-Cl angle of CdCl<sub>2</sub> is 180°, the theoretical calculation of vibration modes was made with Gaussian 03 program. According to this theoretical work, asymmetric Cd-Cl stretching [*v*<sub>as</sub>(Cd-Cl)], symmetrical Cd-Cl stretching [*v*<sub>s</sub>(Cd-Cl)] and in-plane and out-of-plane bending [*β*(Cl-Cd-Cl) ip, *γ*(Cl-Cd-Cl) oop] calculated vibration modes for free CdCl<sub>2</sub> were obtained as unscaled at wavenumbers of 378.26, 292.49 and 66.69 cm<sup>-1</sup>, respectively. It has been observed that these theoretically obtained values are compatible with experimental values [55,56].

In the theoretical calculation for compound **2**, these vibration modes of CdCl<sub>2</sub> bonded to the structure were obtained as unscaled at 354.85, 286.65 and 84.96 cm<sup>-1</sup> wavenumbers, respectively.

#### 4. RESULTS

This study focuses on the molecular structures and chemical properties of [NiCl<sub>2</sub>(2PS)<sub>2</sub>] and [CdCl<sub>2</sub>(pD)]<sub>n</sub> coordination compounds were evaluated by computational and experimental methods. The two compounds crystallized in the Fdd2 and C2/m space groups in orthorhombic and monoclinic crystal systems, respectively. The 2PS ion was attached to the nickel atom from its sulfur atom in the compound **1**. Additionally, the crystal structure of this compound is influenced by π...π interactions among the cage structures of 2PS ions.

In addition, π ... π interactions among the cages structure of 2PS ions contributed to the crystal structure formation. Besides, the pD molecule was attached to the cadmium atoms from its oxygen atoms in the compound **2**. In addition, Cl-Cd-Cl bonds also contributed to the crystal packing of compound **2**.

The Ni(II) ion in compound **1**'s structure is in the center of inversion in a state surrounded by two the sulfur atoms of the 2PS ion and as well as two chlorine atoms. Therefore, the Ni(II) atom displays distorted tetrahedral geometry. In addition, the Cd(II) ion (compound **2**) is in a state surrounded by two oxygen atoms of two pD molecules as well as four chlorine atoms. Thus, the Cd(II) atom exhibits a distorted octahedral geometry.

The compound **1**, we examined is the first and only coordination compound that has bonded to the Ni atom of the 2PS ion only from sulfur atoms. In some future work, new crystals can be obtained with all thiolates and other M(II)Cl<sub>2</sub> structures. The binding patterns and various properties of all thiolates can be studied. Similarly, compound **2**, which we studied, is the first and only coordination compound that is bonded to the Cd atom of the pD molecule only by oxygen atoms. In some future work, new crystals can be obtained with all dioxanes and other M(II)Cl<sub>2</sub> structures. We hope that this study we have done will be a guide for future research in this field.

#### CONFLICTS OF INTEREST

No conflict of interest was declared by the authors.

#### REFERENCES

- [1] Batten, S.R., Champness, N.R., Chen, X.M., Garcia-Martinez, J., Kitagawa, S., Öhrström, L., O'Keeffe, M., Suh, P., Reedijk, J., "Terminology of metal-organic frameworks and coordination polymers (IUPAC Recommendations 2013)", *Pure and Applied Chemistry*, 85(8): 1715-1724, (2013). DOI: <https://doi.org/10.1351/PAC-REC-12-11-20>
- [2] Fromm, K., "Coordination polymer networks with s-block metal ions", *Coordination Chemistry Reviews*; 252 (8-9): 856-885, (2008). DOI: <https://doi.org/10.1016/j.ccr.2007.10.032>
- [3] Yang, Y., Jiang, G., Li, Y.Z., Bai, J., Pan, Y., You, X.Z., "Synthesis, structures and properties of alkaline earth metal benzene-1,4-dioxyacetates with three-dimensional hybrid networks", *Inorganica Chimica Acta*, 359(10): 3257-3263, (2006). DOI: <https://doi.org/10.1016/j.ica.2006.03.038>
- [4] Adams, E.J., Skrydstrup, T., Lindsay, K.B., "2-Pyridinethiol, Encyclopedia of Reagents for Organic Synthesis", (2005). DOI: <https://doi.org/10.1002/047084289X.rp286>
- [5] Shunmugam, R., Sathyanarayana, D.N., "Raman and polarized infrared spectra of pyridine-2-thione", *Spectrochimica Acta Part A: Molecular Spectroscopy*, 40(8):757-761, (1984). DOI: [https://doi.org/10.1016/0584-8539\(84\)80100-2](https://doi.org/10.1016/0584-8539(84)80100-2)

- [6] Castiñiras, A., Hiller, W., Strähle, J., Bravo, J., Casas, J., Gayoso, M., Sordo, J., “Methyl- and phenyl-mercury (II) derivatives of 2-mercaptopyridine. Crystal and molecular structure of methyl(pyridine-2-thiolato) mercury (II)”, *Journal of the Chemical Society, Dalton Transactions*, 9: 1945-1948, (1986). DOI: <https://doi.org/10.1039/dt9860001945>
- [7] Toma, H.E., Santos, P.S., Mattioli, M.P.D., Oliveira, L.A.A., “Kinetics, electrochemistry and resonance raman spectra of the (2-mercaptopyridine) (edta) ruthenium (III) complex”, *Polyhedron*, 6(3): 603-611, (1987). DOI: [https://doi.org/10.1016/S0277-5387\(00\)81031-1](https://doi.org/10.1016/S0277-5387(00)81031-1)
- [8] Baldwin, J.A., Vlčková, B., Andrews, M.P., Butler, S., “Surface-Enhanced Raman Scattering of Mercaptopyridines and Pyrazinamide Incorporated in Silver Colloid-Adsorbate Films”, *Langmuir*, 13(14): 3744-3751, (1997). DOI: <https://doi.org/10.1021/la960719d>
- [9] Pang, Y.S., Hwang, H.J., Kim, M.S., “Adsorption of 2-mercaptopyridine and 2-mercaptopyrimidine on a silver colloidal surface investigated by Raman spectroscopy”, *Journal of Molecular Structure*, 441(1): 63-76, (1998). DOI: [https://doi.org/10.1016/s0022-2860\(97\)00280-9](https://doi.org/10.1016/s0022-2860(97)00280-9)
- [10] Zhang, H.L., Evans, S.D., Henderson, J.R., Miles, R.E., Shen, T.H., “Spectroscopic Characterization of Gold Nanoparticles Passivated by Mercaptopyridine and Mercaptopyrimidine Derivatives”, *The Journal of Physical Chemistry B*, 107(25): 6087-6095, (2003). DOI: <https://doi.org/10.1002/Adma.200390124>
- [11] Ozturk, I.I., Kourkoumelis, N., Hadjikakou, S.K., Manos, M.J., Tasiopoulos, A.J., Butler, I.S., Balzarini, J., Hadjiliadis, N., “Interaction of antimony(III) chloride with thiourea, 2-mercapto-5-methyl-benzimidazole, 3-methyl-2-mercaptobenzothiazole, 2-mercaptopyrimidine, and 2-mercaptopyridine”, *Journal of Coordination Chemistry*, 64(22): 3859-3871, (2011). DOI: <https://doi.org/10.1080/00958972.2011.633603>
- [12] Do, W.H., Lee, C.J., Kim, D.Y., Jung, M.J., “Adsorption of 2-mercaptopyridine and 4-mercaptopyridine on a silver surfaces investigated by SERS spectroscopy”, *Journal of Industrial and Engineering Chemistry*, 18(6): 2141-2146, (2012). DOI: <https://doi.org/10.1016/j.jiec.2012.06.009>
- [13] Naktode, K., Reddy, T.D.N., Nayek, H.P., Mallik, B.S., Panda, T.K., “Heavier group 2 metal complexes with a flexible scorpionate ligand based on 2-mercaptopyridine”, *Royal Society of Chemistry Advances*, 5(63): 51413-51420, (2015). DOI: <https://doi.org/10.1039/C5RA04696C>
- [14] Ramsay, D.A., “The Vibration Spectrum and Molecular Configuration of 1,4-dioxane”, *Proceedings of the Royal Society of London A*, 190: 562-574, (1947). DOI: <https://doi.org/10.1098/rspa.1947.0097>
- [15] Malherbe, F.E., Bernstein, H.J., “The Infrared and Raman Spectra of p-Dioxane”, *Journal of the American Chemical Society*, 74(17): 4408-4410, (1952). DOI: <https://doi.org/10.1021/ja01137a051>
- [16] Snyder, R.G., Zerbi, G., “Vibrational analysis of ten simple aliphatic ethers: Spectra, assignments, valence force field and molecular conformations”, *Spectrochimica Acta Part A: Molecular Spectroscopy*, 23(2): 391-437, (1967). DOI: [https://doi.org/10.1016/0584-8539\(67\)80241-1](https://doi.org/10.1016/0584-8539(67)80241-1)
- [17] Ellestad, O.H., Klaboe, P., Hagen, G., “The vibrational spectra of 1,4-dioxane-d<sub>0</sub> and 1,4-dioxane-d<sub>8</sub>”, *Spectrochimica Acta*, 27A: 1025-1048, (1971). DOI: [https://doi.org/10.1016/0584-8539\(71\)80186-1](https://doi.org/10.1016/0584-8539(71)80186-1)
- [18] Karayannis, N.M., Mikulski, C.M., Specca, A.N., Cronin, J.T., Pytlewski, L.L., “p-Dioxane, p-thioxane, and 1,2-dimethoxyethane complexes with transition metal perchlorates”, *Inorganic Chemistry*, 11(10): 2330-2335, (1972). DOI: <https://doi.org/10.1021/ic50116a008>

- [19] Shimanouchi, T., "Tables of molecular vibrational frequencies consolidated volume II", *Journal of Physical and Chemical Reference Data.*, 6(3): 993-1102, (1977). DOI: <https://doi.org/10.1063/1.555560>
- [20] Schwarz, W., Schmidt, A., Binder, G.E., "1,4-Dioxan·H<sub>2</sub>O·SbCl<sub>5</sub>; Vibrational Spectra, Crystal and Molecular Structure", *Zeitschrift für Naturforschung B*, 33(2): 136-139, (1978). DOI: <https://doi.org/10.1515/znb-1978-0202>
- [21] Dempster, A.B., Uslu, H., "Infrared spectra and stability of Hofmann-type dioxane clathrates", *Spectrochimica Acta Part A: Molecular Spectroscopy*, 34(1): 71-75, (1978). DOI: [https://doi.org/10.1016/0584-8539\(78\)80188-3](https://doi.org/10.1016/0584-8539(78)80188-3)
- [22] Den, H.M., Driessen, W.L., "Ethers as ligands, Part IV, Metal(II) 1,4-dioxane solvates", *Inorganica Chimica Acta*, 39:43-46, (1980). DOI: [https://doi.org/10.1016/s0020-1693\(00\)93631-4](https://doi.org/10.1016/s0020-1693(00)93631-4)
- [23] Parvez, M., Pajerski, A.D., Richey, H.G., "(Dioxane)dineopentylmagnesium: a polymeric structure", *Acta Crystallographica Section C Crystal Structure Communications*, 44(7): 1212-1215, (1998). DOI: <https://doi.org/10.1107/s0108270188003099>
- [24] Edelmann, F.T., Pauer, F., Wedler, M., Stalke, D., "Preparation and structural characterization of dioxane-coordinated alkali metal bis(trimethylsilyl)amides", *Inorganic Chemistry*, 31(20): 4143-4146, (1992). DOI: <https://doi.org/10.1021/ic00046a028>
- [25] Parlak, C., Alver, Ö., "Spectroscopic investigations of 1,4-dioxane adsorbed on bentonite from Anatolia", *Anadolu University Journal of Science and Technology A - Applied Sciences and Engineering*, 17(2): 273-277, (2016). DOI: <https://doi.org/10.18038/btda,87236>
- [26] Borowski, P., Gac, W., Pulay, P., Wolinski, K., "The vibrational spectrum of 1,4-dioxane in aqueous solution – theory and experiment", *New Journal of Chemistry*, 40(9): 7663-7670, (2016). DOI: <https://doi.org/10.1039/c6nj01198e>
- [27] Kartal, Z., Yavuz, A., "The synthesis and the spectroscopic, thermal, and structural properties of the M<sub>2</sub>[(fumarate)Ni(CN)<sub>4</sub>]·2(1,4-Dioxane) clathrate (M = Co, Ni, Cd and Hg)", *Journal of Molecular Structure*, 1155: 171-183, (2018). DOI: <https://doi.org/10.1016/j.molstruc.2017.10.107>
- [28] Lockwood, D.J., Bertrand, D., Carrara, P., Mischler, G., Billerey, D., Terrier, C., "Raman spectrum of NiCl<sub>2</sub>", *Journal of Physics C: Solid State Physics*, 11(17): 3615-3620, (1979). DOI: <https://doi.org/10.1088/0022-3719/12/17/031>
- [29] Agulló-Rueda, F., Calleja, J.M., Martini, M., Spinolo, G., Cariati, F., "Raman and infrared spectra of transition metal halide hexahydrates", *Journal of Raman Spectroscopy*, 18(7): 485-491, (1987). DOI: <https://doi.org/10.1002/jrs.1250180707>
- [30] Lide, D.R., "CRC Handbook of Chemistry and Physics", 90th ed, Boca Raton, Florida, USA: CRC Press, ISBN 978-1-4200-9084-0, (2009).
- [31] Seidell, A., "Solubilities of Inorganic and Organic Compounds: A Compilation of Quantitative Solubility Data From the Periodical Literature; Volume 1", Legare Street Press, ISBN-10: 1015948987, (2022).
- [32] Greenwood, N.N., Earnshaw, A., "Chemistry of the Elements", Second Edition, Butterworth-Heinemann, Oxford, UK: ISBN: 9780750633659. (1997).



- [33] Wells, A.F., "Structural Inorganic Chemistry", Fourth Edition, Oxford University Press, Oxford, UK: ISBN: 0198553544, (1975).
- [34] Smith, M.B., March, J., "March's Advanced Organic Chemistry: Reactions, Mechanisms, and Structure", 6th ed., Wiley, New York, USA: ISBN-10: 0471720917, (2007).
- [35] Frisch, M.J., Trucks, G.W., Schlegel, H.B., Scuseria, G.E., Robb, M.A., Cheeseman, J.R., Montgomery, Jr.J.A., Vreven, T., Kudin, K.N., Burant, J.C., Millam, J.M., Iyengar, S.S., Tomasi, J., Barone, V., Mennucci, B., Cossi, M., Scalmani, G., Rega, N., Petersson, G.A., Nakatsuji, H., Hada, M., Ehara, M., Toyota, K., Fukuda, R., Hasegawa, J., Ishida, M., Nakajima, T., Honda, Y., Kitao, O., Nakai, H., Klene, M., Li, X., Knox, J.E., Hratchian, H. P., Cross, J.B., Bakken, V., Adamo, C., Jaramillo, J., Gomperts, R., Stratmann, R.E., Yazyev, O., Austin, A.J., Cammi, R., Pomelli, C., Ochterski, J.W., Ayala, P.Y., Morokuma, K., Voth, G.A., Salvador, P., Dannenberg, J.J., Zakrzewski, V.G., Dapprich, S., Daniels, A.D., Strain, M.C., Farkas, O., Malick, D.K., Rabuck, A.D., Raghavachari, K., Foresman, J.B., Ortiz, J.V., Cui, Q., Baboul, A.G., Clifford, S., Cioslowski, J., Stefanov, B.B., Liu, G., Liashenko, A., Piskorz, P., Komaromi, I., Martin, R.L., Fox, D.J., Keith, T., Al-Laham, M.A., Peng, C.Y., Nanayakkara, A., Challacombe, M., Gill, P.M.W., Johnson, B., Chen, W., Wong, M.W., Gonzalez, C., Pople, J.A., Gaussian 03 Revision D.01. Gaussian, Inc., Wallingford CT, (2004).
- [36] Young, D.C., "Computational chemistry: a practical guide for applying techniques to real-world problems (electronics)", New York, USA: Wiley, ISBN: 0-471-33368-9, (2001).
- [37] Dennington, R., Keith, T., Millam, J., Gauss View, Version 4.1.2. Semichem Inc., Shawnee Mission (2007).
- [38] Sheldrick, G.M., "A short history of SHELX", *Acta Crystallographica*, A64: 112-122, (2008). DOI: <https://doi.org/10.1107/S0108767307043930>
- [39] Farrugia, L.J., "WinGX and ORTEP for Windows: an update", *Journal of Applied Crystallography*, 45: 849-854, (2012). DOI: <https://doi.org/10.1107/S0021889812029111>
- [40] Macrae, C.F., Bruno, I.J., Chisholm, J.A., Edgington, P., McCabe, P., Pidcock, E., Rodriguez-Monge, L., Taylor, R., van de Streek, J., Wood, P.A., "Mercury CSD 2.0 – New features for the visualization and investigation of crystal structures", *Journal of Applied Crystallography*, 41: 466-470, (2008). DOI: <https://doi.org/10.1107/S0021889807067908>
- [41] Sickerman, N.S., Park, Y.J., Ng, G.K.Y., Bates, J.E. Hilkert, M., Ziller, J.W., Furche, F., Borovik, A.S., "Synthesis, structure, and physical properties for a series of trigonal bipyramidal M(II)-Cl complexes with intramolecular hydrogen bonds", *Dalton Transactions*, 41(15): 4358-4364, (2012). DOI: <https://doi.org/10.1039/c2dt12244h>
- [42] Gusev, A.N., Shul'gin, V.F., Ryush, I.O., Hasegawa, M., Kiskin, M.A., Efimov, N.N., Konstantin, A., Lyssenko, A., Eremenko, I.L., Linert, W., "Copper(II), Nickel(II), and Cobalt(II)/(III) Self-Assembled Polynuclear Complexes of Bis[(pyridin-2-yl)-1,2,4-triazol-3-yl]methane", *European Journal of Inorganic Chemistry*, 3: 704-712, (2017). DOI: <https://doi.org/10.1002/ejic.201601107>
- [43] Paes, L.W.C., Suárez, J.A., Márquez, A.M., Sanz, J.F., "First-principles study of nickel complex with 1,3-dithiole-2-thione-4,5-dithiolate ligands as model photosensitizers", *Theoretical Chemistry Accounts*, 136(6): 1-9, (2017). DOI: <https://doi.org/10.1007/s00214-017-2098-7>
- [44] Hakimi, M., Mardani, Z., Moeini, K., Fernandes, M.A., "Coordination geometries and crystal structures of cadmium(II) complexes with a new amino alcohol (NN'O) ligand", *Journal of*

- Coordination Chemistry, 65(13): 2221-2233, (2012). DOI: <https://doi.org/10.1080/00958972.2012.690145>
- [45] Kawasaki, T., Kitazawa, T., "Synthesis and Crystal Structures of Cadmium(II) Cyanide with Branched-Butoxyethanol", Crystals, 8(5): 221/1-221/10, (2018). <https://doi.org/10.3390/cryst8050221>
- [46] BelhajSalah, S., Abdelbaky, M.S.M., García-Granda, S., Essalah, K., Ben Nasr, C., Mrad, M.L., "Crystal structure, Hirshfeld surfaces computational study and physicochemical characterization of the hybrid material (C<sub>7</sub>H<sub>10</sub>N)<sub>2</sub>[SnCl<sub>6</sub>]·H<sub>2</sub>O", Journal of Molecular Structure, 1152: 276-286, (2018). DOI: <https://doi.org/10.1016/j.molstruc.2017.09.098>
- [47] Jellali, A., Elleuch, S., Hamdi, B., Zouari, R., "Experimental and theoretical investigations of the molecular structure, the spectroscopic properties and TD-DFT analysis of a new semiconductor hybrid based iron (III)", Journal of Saudi Chemical Society, 23(5): 600-611, (2019). DOI: <https://doi.org/10.1016/j.jscs.2018.10.006>
- [48] Zhang, W., Schmid, T., Yeo, B.S., Zenobi, R., "Tip-enhanced Raman spectroscopy reveals rich nanoscale adsorption chemistry of 2-mercaptopyridine on Ag", Israel Journal of Chemistry, 47(2): 177-184, (2007). DOI: <https://doi.org/10.1560/ijc.47.2.177>
- [49] Kartal, Z., Sayın, E., "FTIR spectroscopic and thermal study of M(Cyclohexanethiol)<sub>2</sub>Ni(CN)<sub>4</sub>·(1,4-dioxane) clathrate (M = Mn, Co, Ni and Cd)", Journal of Molecular Structure, 994(1-3): 170-178, (2011). DOI: <https://doi.org/10.1016/j.molstruc.2011.03.014>
- [50] Kartal, Z., Türk, T., "FT-IR spectroscopic and thermal study of M(1,6-hexanedithiol)Ni(CN)<sub>4</sub>·2(1,4-dioxane) clathrate (M = Mn, Co, Ni and Cd)", Journal of Molecular Structure, 1014: 74-80, (2012). DOI: <https://doi.org/10.1016/j.molstruc.2012.01.031>
- [51] Eckert, S., Miedema, P.S., Quevedo, W., O'Conneide, B., Fondell, M., Beye, M., Pietzsch, A., Ross, M., Khalil, M., Föhlich, A., "Molecular structures and protonation state of 2-Mercaptopyridine in aqueous solution", Chemical Physics Letters, 647: 103-106, (2016). DOI: <https://doi.org/10.1016/j.cplett.2016.01.050>
- [52] Do, W.H., Lee, C.J., Kim, D.Y., Jung, M.J., "Adsorption of 2-mercaptopyridine and 4-mercaptopyridine on a silver surfaces investigated by SERS spectroscopy", Journal of Industrial and Engineering Chemistry, 18(6): 2141-2146, (2012). DOI: <https://doi.org/10.1016/j.jiec.2012.06.009>
- [53] Jamroz, M.H., "Vibrational Energy Distribution Analysis VEDA 4", Warsaw, (2004-2010).
- [54] Solomons, T.W.G., Fryhle, C.B., Scott, A., "Organic Chemistry", New York, USA: Wiley, ISBN 10: 1119768195, (2022).
- [55] Lockwood, D.J., "Raman Spectra of Cadmium Chloride and Cadmium Bromide. In: G.B. Wright (eds) Light Scattering Spectra of Solids", Springer, Berlin, Heidelberg, (1969). DOI: [https://doi.org/10.1007/978-3-642-87357-7\\_6](https://doi.org/10.1007/978-3-642-87357-7_6)
- [56] Lockwood, D.J., "Lattice vibrations of CdCl<sub>2</sub>, CdBr<sub>2</sub>, MnCl<sub>2</sub>, and CoCl<sub>2</sub>: infrared and Raman spectra", Journal of the Optical Society of America, 63: 374-382, (1973). DOI: <https://doi.org/10.1364/JOSA.63.000374>

## APPENDIX

**Table S1.** Experimental FT-IR modes of 2MP and NiCl<sub>2</sub> in solid state with theoretical and experimental vibration modes of compound **1**

Experimental FT-IR modes and assignment of 2MP*	Theoretical vibration modes of <b>1</b>		Experimental FT-IR modes of <b>1</b>	Assignments and PED (%)**
	Unscaled	Scaled		
<b>3160</b> v(CH)	<b>3251</b>	<b>3153.47</b>	<b>3173</b>	<b>v(CH) 85</b>
<b>3099</b> v(CH)	<b>3241</b>	<b>3143.77</b>	<b>3113</b>	<b>v(CH) 90</b>
<b>3048</b> v(CH)	<b>3223</b>	<b>3126.31</b>	<b>3077</b>	<b>v(CH) 91</b>
<b>3021</b> v(CH)	<b>3214</b>	<b>3117.58</b>	<b>3038</b>	<b>v(CH) 96</b>
<b>2507</b> v(SH)	-	-	-	-
<b>1574</b> v(C=C)	<b>1594</b>	<b>1578.06</b>	<b>1605</b>	<b>v(CC) 60</b>
-	1585	1569.15	1581	v(CC) 40
1489 n. a.	1464	1449.36	-	β(HCN) 70
<b>v(C=C), v(C=N)</b>	<b>1444</b>	<b>1428.57</b>	<b>1443</b>	<b>β(HCC) 62</b>
-	1318	1304.82	-	v(NC) 51
-	1311	1297.89	1293	v(NC) 26 β(HCN) 26
1234 n. a.	1198	1186.02	1229	β(HCC) 80
<b>1123</b> β(C-S) ip / Ring breathing	<b>1122</b>	<b>1110.78</b>	<b>1107</b>	<b>v(CC) 20 β(HCC) 21</b>
-	1094	1083.06	1084	-
-	1053	1042.47	-	v(CC) 58
-	1049	1038.51	1031	τ(HCCC) 36 τ(HCCN) 24
995 Ring breathing	1007	996.93	997	τ(HCCS) -11 τ(HCNC) 38 τ(HCCC) 10
976 β(CH) ip	978	968.22	969	β(CCC) 32
-	932	922.68	938	τ(HCCS) 18 τ(HCNC) 42 τ(HCCC) -18
<b>900</b> β(C-SH) ip	-	-	-	-
807 n. a.	809	800.91	819	τ(HCCC) 24 τ(CCNC) 11
-	763	755.37	757	τ(HCCN) 20 τ(CNCC) -13 τ(CCNC) -17
<b>739</b> v(C-S)	<b>725</b>	<b>717.75</b>	<b>723</b>	<b>v(SC) 33 β(CCC) 43</b>
618 β(CCC) ip / Ring twisting	624	617.76	618	β(CNC) -22 β(NCC) 18 β(CCN) 18
482 n. a.	500	495.00	517	τ(CCCC) -10 τ(CCCN) 17 τ(SCNC) -22
442 β(C-S) oop / β(CCC) ip	443	438.57	<b>442</b>	<b>v(NiCl) 90</b>
-	424	419.76	-	τ(CCCC) 32 τ(CNCC) -10
-	407	402.93	-	v(SC) 42
-	<b>325</b>	<b>321.75</b>	-	<b>v(NiS) 70</b>

-	<b>304</b>	<b>300.96</b>	-	<b><i>v(NiCl)</i> 96</b>
-	280	277.20	-	$\beta$ (NCS) 30 $\beta$ (SCN) 36
<b>212 <math>\beta</math>(C-SH) oop</b>	-	-	-	-
-	190	188.10	-	$\beta$ (CSNi) -12 $\beta$ (NiSC) 12 $\tau$ (NCCC) 16 $\tau$ (CNCS) 14
-	135	133.65	-	$\tau$ (CISCINi) 76
-	124	122.76	-	$\beta$ (CINiCl) 72 $\beta$ (SNiS) -10
-	107	105.93	-	$\beta$ (CINiS) -28 $\tau$ (CISSNi) 61
-	<b>88</b>	<b>87.12</b>	-	<b><i>B(SNiS)</i> 57</b>
-	<b>82</b>	<b>81.18</b>	-	<b><i>B(CINiS)</i> 47 <i>B(CINiCl)</i> -12</b>
-	55	54.45	-	$\beta$ (CSNi) 29 $\tau$ (CNCS) 21
-	39	38.61	-	$\tau$ (NCSNi) 34 $\tau$ (CSNiS) -12 $\tau$ (SNiSC) 12 $\tau$ (NiSCC) 36
-	23	22.77	-	$\tau$ (NCSNi) 11 $\tau$ (NiSCC) -10

v: stretching,  $v_a$ : asymmetric stretching,  $v_s$ : symmetric stretching,  $\beta$ : bending,  $\tau$ : torsion, ip: in plane, oop: out of plane, n. a.: not assigned, PED: Potential Energy Distribution, + values: for symmetric modes, - values: asymmetric modes. Percentage contributions of the PED values of each mode are given only for values greater than 20% or the highest percentage value for that mode for values less than 20%.

\*: Taken reference [12],

\*\* : The 53<sup>rd</sup> reference is taken as the source.

**Table S2.** Experimental FT-IR modes of pD with theoretical and experimental vibration modes of compound 2

Experimental FT-IR modes and assignments of pD*	Theoretical vibration modes of 2		Experimental FT-IR modes of 2	Assignments and PED (%)**
	Unscaled	Scaled		
-	3171.12 (IR, Ra)	2958.66	3026	$\nu(\text{CH})$ 37 $\nu(\text{CH})$ 35
-	3169.42 (Ra)	2957.07	-	$\nu(\text{CH})$ -35 $\nu(\text{CH})$ 38
-	3157.19 (Ra)	2945.66	-	$\nu(\text{CH})$ -44 $\nu(\text{CH})$ -44
-	3154.48 (Ra)	2943.13	-	$\nu(\text{CH})$ -44 $\nu(\text{CH})$ 44
-	3081.79 (Ra)	2875.31	-	$\nu(\text{CH})$ 38 $\nu(\text{CH})$ 36
-	3079.34 (IR, Ra)	2873.02	2991	$\nu(\text{CH})$ -37 $\nu(\text{CH})$ 38
<b>2961 <math>\nu_{\text{as}}(\text{CH})</math> (equatorial)</b>	<b>3043.34 (IR, Ra)</b>	<b>2839.44</b>	<b>2951</b>	<b><math>\nu(\text{CH})</math> 45 <math>\nu(\text{CH})</math> 45</b>
2854 $\nu_{\text{s}}(\text{CH})$ (axial)	3038.71 (IR, Ra)	2835.12	2859	$\nu(\text{CH})$ 45 $\nu(\text{CH})$ -45
-	-	-	1625	
-	-	-	1584	
-	1511.81 (IR, Ra)	1496.69	-	$\beta(\text{HCH})$ -36 $\beta(\text{HCH})$ -41
-	1502.54 (IR)	1487.30	-	$\beta(\text{HCH})$ -38 $\beta(\text{HCH})$ -40
-	1502.32 (IR, Ra)	1487.29	-	$\beta(\text{HCH})$ -44 $\beta(\text{HCH})$ 42
<b>1453 <math>\text{CH}_2</math> sym. deformation</b>	<b>1494.28 (IR, Ra)</b>	<b>1479.34</b>	<b>1431</b>	<b><math>\beta(\text{HCH})</math> -45 <math>\beta(\text{HCH})</math> 43</b>
1445 $\text{CH}_2$ sym. deformation	1414.37 (Ra)	1400.23	-	$\tau(\text{HCOC})$ 22
-	1412.60 (Ra)	1398.47	-	$\tau(\text{HCOC})$ 23
-	1389.38 (IR)	1375.49	-	$\tau(\text{HCOC})$ 15
1375 $\text{CH}_2$ wagging	1378.16 (IR, Ra)	1364.39	1373	$\tau(\text{HCOC})$ 19
1366 $\text{CH}_2$ wagging + CC stretch	1326.18 (Ra)	1312.92	-	$\beta(\text{HCO})$ -24 $\beta(\text{HCO})$ 31
-	1301.22 (IR, Ra)	1288.21	1283	$\beta(\text{HCO})$ -27 $\beta(\text{HCO})$ 29
<b>1289 <math>\text{CH}_2</math> twisting</b>	<b>1274.70 (IR)</b>	<b>1261.95</b>	<b>1256</b>	<b><math>\beta(\text{HCO})</math> -19</b>
1255 $\text{CH}_2$ twisting	1225.81 (Ra)	1213.55	-	$\beta(\text{HCO})$ 22 $\beta(\text{HCO})$ -25 $\beta(\text{HCO})$ -20
-	1146.40 (Ra)	1134.94	-	$\tau(\text{COCC})$ -22 $\tau(\text{COCC})$ -22
<b>1122 COC asym. stretch</b>	<b>1119.47 (IR)</b>	<b>1108.28</b>	<b>1110</b>	<b><math>\nu(\text{OC})</math> 29 <math>\nu(\text{OC})</math> -21</b>
1084 $\text{CH}_2$ rocking	1097.55 (IR)	1086.57	1076	$\nu(\text{OC})$ -17
-	1055.47 (IR)	1044.92	-	$\nu(\text{OC})$ 37 $\nu(\text{OC})$ -22
1048 ring trigonal def.	1049.11 (IR, Ra)	1038.62	-	$\beta(\text{COC})$ 22
-	1026.22 (IR, Ra)	1015.96	1031	$\nu(\text{CC})$ 44
888 CC stretch	893.44 (IR)	884.51	888	$\beta(\text{OCC})$ 23

<b>874 COC sym. stretch</b>	<b>849.81 (IR, Ra)</b>	<b>841.31</b>	<b>850</b>	<b>v(OC) 23</b>
-	826.56 (IR)	818.29	-	v(OC) 24 v(OC) 22
-	802.56 (IR, Ra)	794.53	-	v(OC) 26
<b>614 CH<sub>2</sub> rocking + ring def.</b>	<b>608.43 (IR)</b>	<b>602.35</b>	<b>621</b>	<b><math>\beta</math>(COC) -21</b>
-	471.99 (Ra)	467.27	-	$\beta$ (OCC) 23 $\beta$ (OCC) -20
-	<b>451.61 (IR, Ra)</b>	<b>447.09</b>	-	<b>v(CdO) 13 <math>\beta</math>(COC) 26</b>
-	402.32 (IR, Ra)	398.30	-	$\beta$ (COC) 14
-	<b>354.85 (IR)</b>	<b>351.30</b>	-	<b>v(CdCl) 49 v(CdCl) -49</b>
-	<b>286.65 (IR, Ra)</b>	<b>283.78</b>	-	<b>v(CdCl) 50 v(CdCl) 50</b>
-	274.89 (IR)	272.14	-	$\tau$ (COCC) -19
-	259.17 (IR)	256.58	-	$\beta$ (CdOC) 22 $\tau$ (OCCO) 34
-	<b>172.88 (IR)</b>	<b>171.15</b>	-	<b>v(CdO) 76</b>
-	140.67 (IR, Ra)	139.26	-	$\beta$ (CdOC) 67
-	<b>84.96 (IR)</b>	<b>84.11</b>	-	<b><math>\beta</math>(ClCdCl) 93</b>
-	72.58 (IR)	71.85	-	$\tau$ (ClOClCd) oop -83
-	69.73 (IR, Ra)	69.03	-	$\beta$ (ClCdO) 81
-	41.23 (IR)	40.82	-	$\tau$ (CdCCO) oop 79
-	34.08 (IR, Ra)	33.74	-	$\tau$ (ClCdOC) -90

v: stretching,  $v_a$ : asymmetric stretching,  $v_s$ : symmetric stretching,  $\beta$ : bending,  $\tau$ : torsion, ip: in plane, oop: out of plane, n. a.: not assigned, PED: Potential Energy Distribution, + values: for symmetric modes, - values: asymmetric modes. Percentage contributions of the PED values of each mode are given only for values greater than 20% or the highest percentage value for that mode for values less than 20%.

\*: Taken from reference [26].

\*\* : The 53<sup>rd</sup> reference is taken as the source.

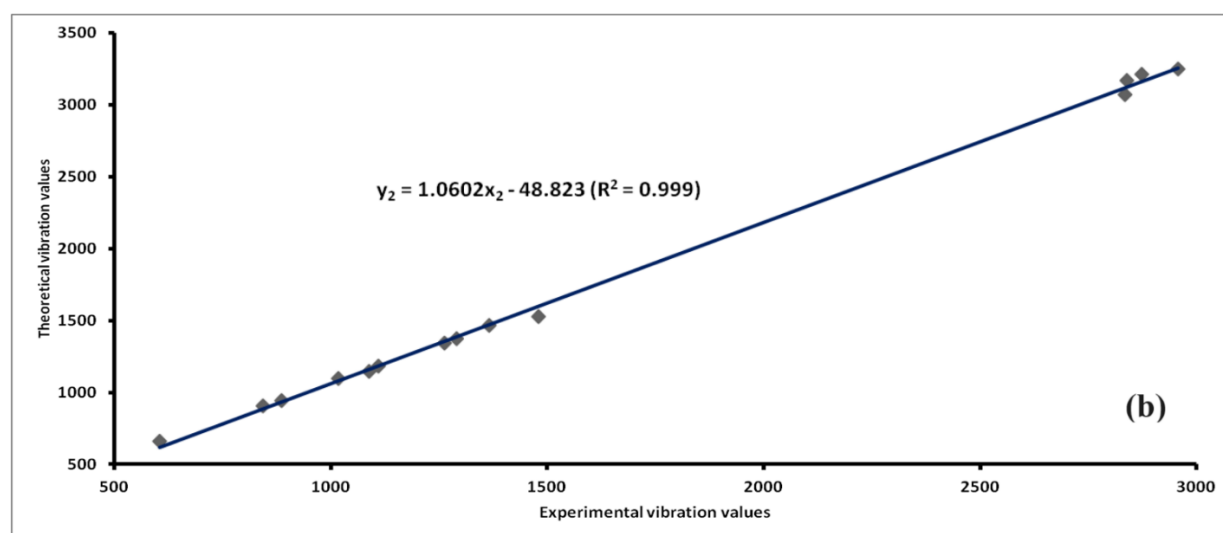
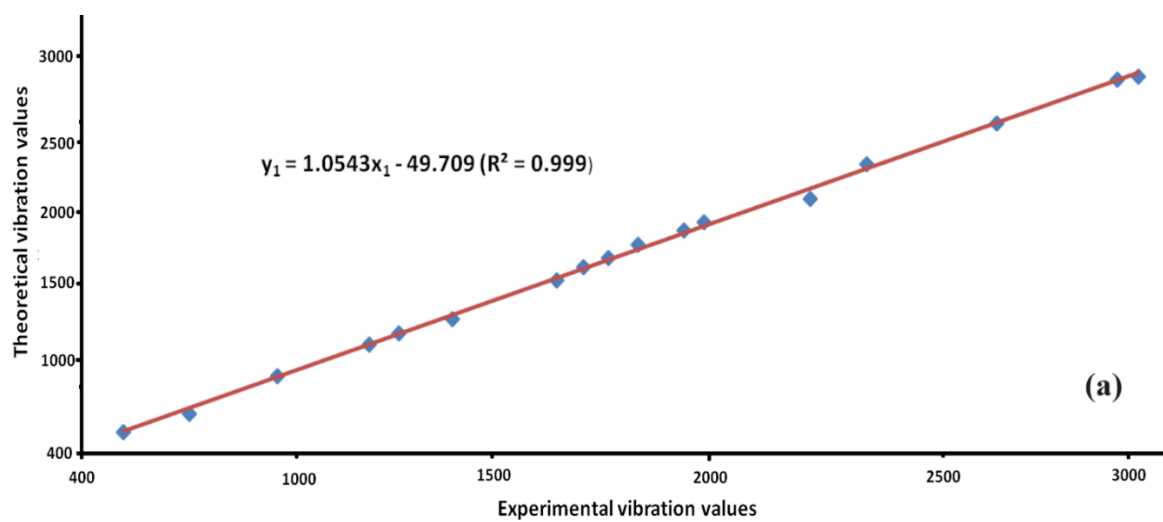


**Figure S1.** Graphs showing the relationships between the experimental vibrational wavenumbers and the theoretically calculated vibrational wavenumbers of compounds **1** (a) and **2** (b)

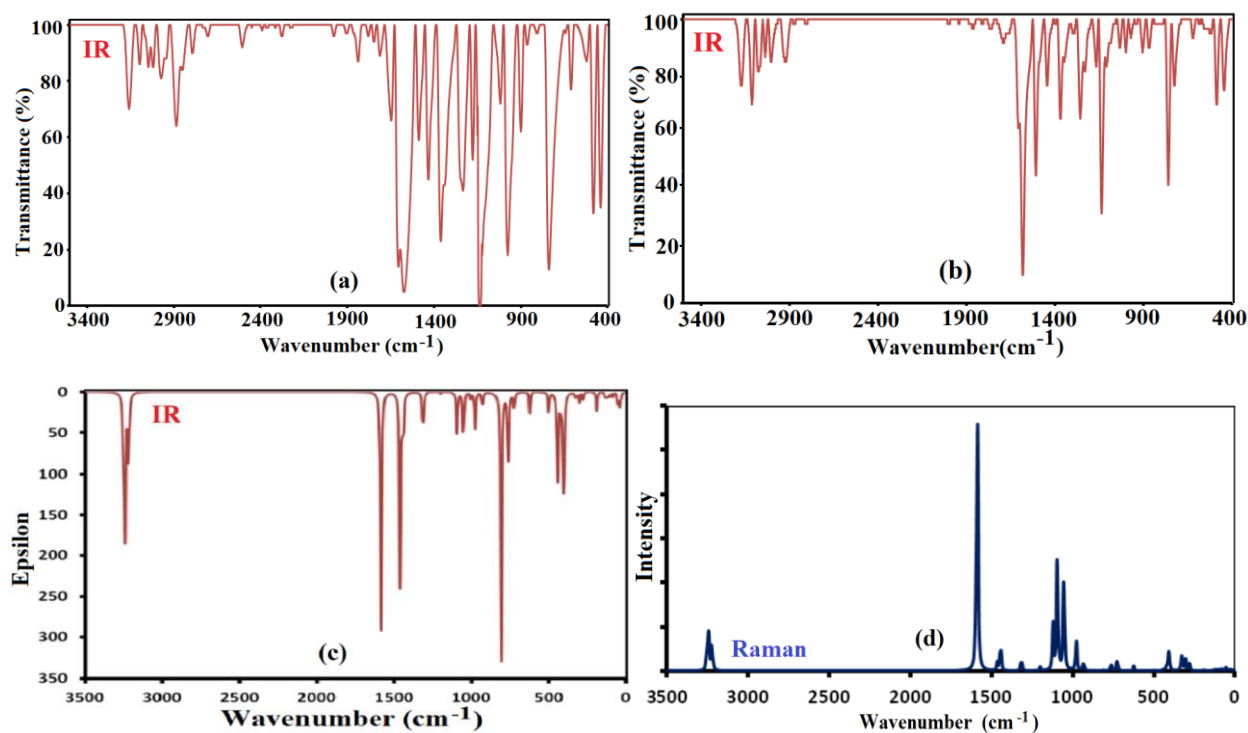


**Figure S2.** FT-IR spectrum of solid state 2MP (a), experimental FT-IR spectrum of compound 1 (b), and theoretical vibration spectra of compound 1; FT-IR spectrum (c) and FT-Raman spectrum (d)



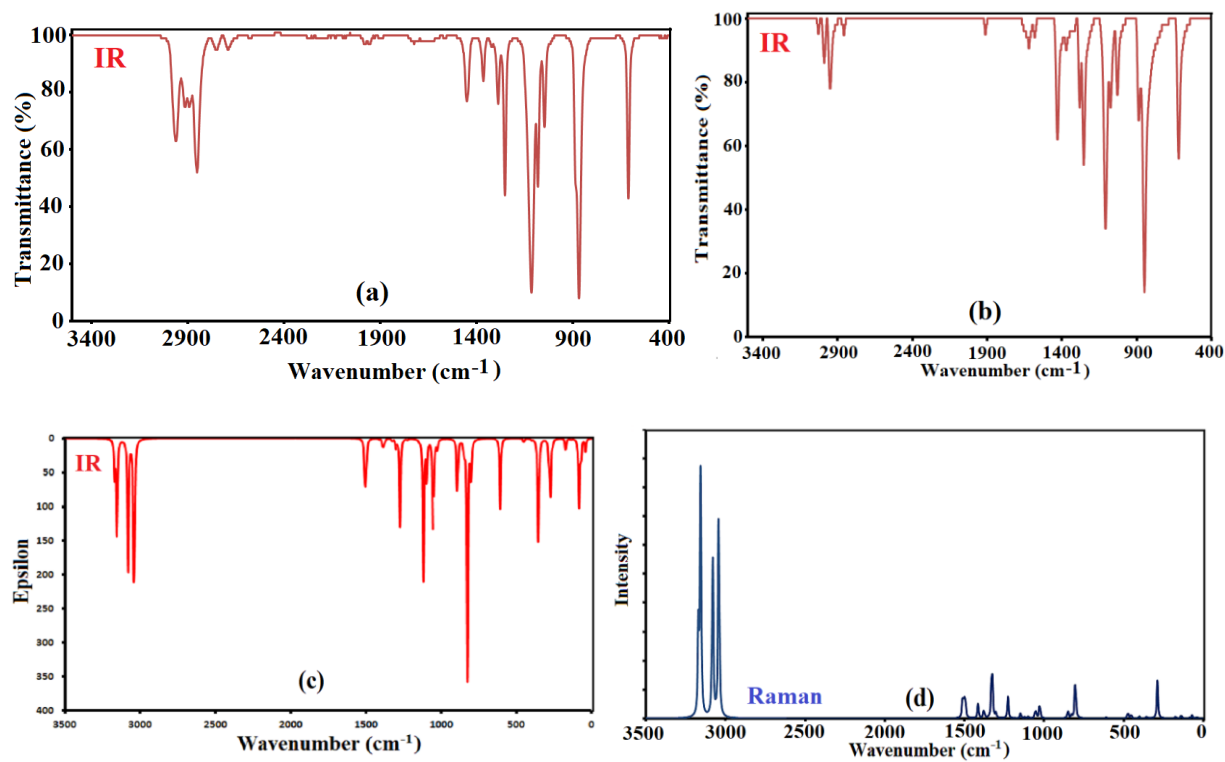


**Figure S3.** FT-IR spectrum of liquid state pD (a), experimental FT-IR spectrum of compound 2 (b), and theoretical vibration spectra of compound 2; FT-IR spectrum (c) and FT-Raman spectrum (d)